Eur. Phys. J. B **53**, 23–28 (2006)
DOI: 10.1140/epjb/e2006-00340-5

**THE EUROPEAN PHYSICAL JOURNAL B**

# Spectroscopy of $La_{0.5}Sr_{1.5}MnO_4$ orbital ordering: a cluster many-body calculation

A. Mirone[1,a], S.S. Dhesi[2], and G. van der Laan[3]

[1] European Synchrotron Radiation Facility, BP 220, 38043 Grenoble Cedex, France
[2] Diamond Light Source, Chilton, Didcot, OX11 0DE, UK
[3] CCLRC Daresbury Laboratory, Warrington WA4 4AD, UK

Received 24 February 2006 / Received in final form 19 July 2006
Published online 6 September 2006 – 

**Abstract.** Orbital ordering (OO) in $La_{0.5}Sr_{1.5}MnO_4$ has been studied using soft X-ray resonant diffraction (SXRD) at the Mn $L_{2,3}$ edges in combination with many-body cluster calculations. The SXRD intensity is modelled in second quantization using a small planar cluster consisting of a central active Mn site with first-neighbour shells comprising O and Mn sites. The effective Hamiltonian includes Slater-Koster parameters and charge transfer and electron correlation energies obtained from previous measurements on manganites. The energy dependence of the SXRD OO peak is calculated using the Jahn-Teller distortions of the oxygen octahedra and in-plane spin correlations as adjustable parameters. These contributions are clearly distinguished above the Néel temperature with a good spectroscopic agreement. The results also suggest a significant charge separation between the Mn sites.

**PACS.** 61.10.-i X-ray diffraction and scattering – 71.30.+h Metal-insulator transitions and other electronic transitions – 71.10.-w Theories and models of many-electron systems – 78.20.Bh Theory, models, and numerical simulation

## 1 Introduction

Orbital ordering (OO), involving a spatial redistribution of valence states, has attracted renewed interest in recent years, even though it has been studied since the predictions of Goodenough over 50 years ago [1]. In the original model Goodenough proposed that the Mn ions in manganites are present in two distinct charge states which allows the possibility of OO influencing the magnetic ordering [1]. For $La_{0.5}Sr_{1.5}MnO_4$ the Mn sites can be considered to have an average valence of +3.5 at room temperature, but below the charge ordering (CO) temperature ($T_{\mathrm{CO}}$) of ∼217 K two inequivalent sites have been proposed. The degeneracy in the valence states of one of these sites can then be lifted by Jahn-Teller (JT) distortion of the oxygen octahedra or by antiferromagnetic spin ordering leading to orbital ordering (OO). In the case of $La_{0.5}Sr_{1.5}MnO_4$ the OO temperature ($T_{\mathrm{OO}}$) is equivalent to $T_{\mathrm{CO}}$. On further cooling below the Néel temperature ($T_{\mathrm{N}}$) of ∼120 K a long-range CE-type antiferromagnetic structure develops.

The $MnO_2$ plane in $La_{0.5}Sr_{1.5}MnO_4$ with its OO super-structure is displayed in Figure 1 [2–7]. The two charge-separated Mn sites, which are denoted $Mn^{3+}$ and $Mn^{4+}$ (although the charge separation is fractional) display a checker board pattern. One can see ferromagnetic zig-zag chains, where the $Mn^{4+}$ sites form the corners and the $Mn^{3+}$ sites are in the middle of the straight segments. Adjacent zig-zag chains are antiferromagnetically aligned with respect to each other. There is a JT distortion of the O atoms consisting of an elongation of the $Mn^{3+}$–O bonds along the zig-zag segments. Figure 1 shows the occupied $Mn^{3+}$ $e_g$ orbital under the hypothesis of $3z^2-r^2/3x^2-r^2$ ordering, which is a possible simplified way of looking at the electronic structure, although so far there is not yet a consensus regarding the correct ordering. More importantly, there is no consensus regarding the interplay between the OO and the in-plane spin correlation for the temperature range $T_{\mathrm{N}} < T < T_{OO}$, even though there is evidence to suggest that short-range in-plane magnetic correlations above $T_{\mathrm{N}}$ are important [8–10].

X-ray resonant diffraction (XRD) at the Mn $K$-edge has been used to directly observe OO in $La_{0.5}Sr_{1.5}MnO_4$, but the $1s \rightarrow 4p$ transitions do not directly probe the $3d$ states involved in OO and consequently the results are controversial [11–16]. This is mainly because XRD at the Mn $K$-edge does not clearly distinguish between OO due to JT distortion and OO due to magnetic correlation [17–19]. On the other hand, soft X-ray resonant diffraction (SXRD) using the huge $2p \rightarrow 3d$ electric-dipole transitions provides a direct probe to study the states involved in OO, and by comparing the incident photon energy dependence of the OO SXRD intensity

[a] e-mail: mirone@esrf.fr

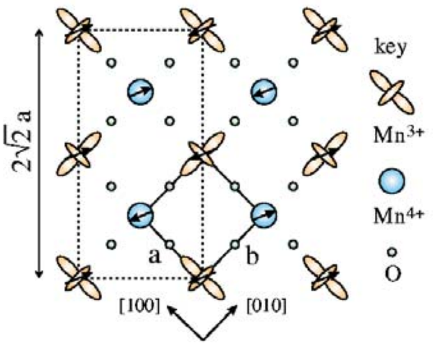


**Fig. 1.** The magnetic unit cell in the $MnO_2$ plane of $La_{0.5}Sr_{1.5}MnO_4$ and its OO super structure shown by the dashed rectangle. The arrows indicate the spin direction, i.e. the $\hat{z}$ direction.

with ligand-field calculations some distinction between the two different contributions can be made [17–19]. Even in the absence of theoretical calculations a great deal can be revealed using SXRD alone. Staub et al. [8] recently used azimuthal scans and polarisation analysis of the OO diffraction peak intensity to demonstrate that there is a significant magnetic contribution to the OO spectrum, as opposed to enhanced contributions from JT distortion, below $T_{\mathrm{N}}$.

The SXRD OO energy dependent spectrum shows a strong multiplet structure due to electric-dipole transitions $3d^n \leftrightarrow 2p^5 3d^{n+1}$ [20], which on the one hand complicates the analysis but on the other hand allows for a much deeper analysis. Previous studies [7,8,17,19] simplified the analysis of the multiplet structure by considering integer charge ordering with a $3d$ occupation of 4 electrons on the active sites (i.e. active in the OO diffraction process). The scattering factors of the active $Mn^{3+}$ sites were then calculated using the crystal-field approximation. Although such calculations were able to reproduce some features of the observed spectrum, the agreement was not good enough to clearly discriminate between several hypotheses concerning the occupied orbitals [17–19]. Moreover, these calculations were based on a local mean-field approximation and were therefore unable to treat the effects of spin correlation between the different Mn sites. The approximation of integer occupation also contrasts with results from band-structure calculations, which are estimating the charge separation between the two Mn sites to be about 0.3 electrons instead of one electron [21]. Therefore, the degree of charge separation remains a controversial issue both experimentally and theoretically [22,23].

In this work we go beyond the limitations of previous work based on ligand-field calculations by building a cluster around the active $Mn^{3+}$ site. We consider a degenerate $3d$ shell on the active $Mn^{3+}$ site, which is coupled to the neighbouring O orbitals by hopping terms. In turn, the O orbitals are coupled to the $3d$ orbitals of the inactive $Mn^{4+}$ sites which, on symmetry grounds, do not contribute to the OO diffraction peak. For the inactive $Mn^{4+}$ site only one $e_g$ orbital is considered with a spin-dependent energy term. In this model, the JT distortion of the oxygen sites and the spin magnetization of the inactive $Mn^{4+}$ sites are explored as adjustable parameters.

In Section 2 we define the Hamiltonian and in Section 3 we fix the parameters. In Section 4 we compare the experimental spectra to the calculated spectra obtained by choosing an optimal distortion. The study of the dependence of the calculated spectra on distortion and spin magnetization is summarized in Section 5.

## 2 Model Hamiltonian

We consider a model where the degenerate $3d$ electrons of the active site are coupled to the neighbouring oxygen orbitals by a hopping term modulated by Slater-Koster parameters. The oxygen orbitals are in turn coupled to the $3d$ orbitals of the inactive $Mn^{4+}$ sites. The Hamiltonian of the total system is

$$H = H_a + H_1 + H_2 + T_1 + T_2\,, \tag{1}$$

where $H_a$ is the atomic Hamiltonian for the active Mn site and $H_1$ and $H_2$ are the Hamiltonians for the first-neighbour O atoms and the neighbouring inactive $Mn^{4+}$ sites, respectively, in the absence of hopping. The $T_1$ and $T_2$ are hopping terms for the $Mn^{3+}$–O and O–$Mn^{4+}$ bonds, respectively.

$$T_1 = \sqrt{2}\,t \sum_\sigma \left(g\, o^\dagger_{x,\sigma} d_{x^2,\sigma} + o^\dagger_{z,\sigma} d_{z^2,\sigma} + o^\dagger_{y,\sigma} d_{y^2,\sigma}\right) + \text{c.c.}, \tag{2}$$

where the local $z$ and $x$ axes lie in the $MnO_2$ plane, $t$ is the Slater-Koster $V_\sigma$ parameter, $g$ is the reduction factor of the hopping along $x$ (which is taken parallel to the straight segment of the zig-zag). The $d$ and $o$ are second-quantization operators for Mn $3d$ and O $2p$ electrons, respectively. Neglecting the smaller $V_\pi$ parameter, we consider only three O orbitals (six including spin) and $o_{x,y,z}$ represents the orbitals in the $x, y, z$ directions. Only one O per direction is considered and a factor $\sqrt{2}$ is included in $T_1$, so that the $o$-s represent symmetrised orbitals. The $d_{x^2}$, $d_{y^2}$ and $d_{z^2}$ are linear combinations of $e_g$ operators pointing along the three Cartesian directions (e.g., $d_{x^2} = \sqrt{3}/2\, d_{x^2-y^2} - 1/2\, d_{z^2}$). The $o_z$ and $o_x$ degrees of freedom are in turn coupled to two $Mn^{4+}$ sites by a hopping term

$$T_2 = t \sum_\sigma \left(o^\dagger_{x,\sigma} X_\sigma + o^\dagger_{z,\sigma} Z_\sigma\right) + \text{c.c.}, \tag{3}$$

where $X(Z)$ represents an $e_g$ orbital at the $Mn^{4+}$ site along the local $x(z)$ direction.

The Hamiltonian $H_1$ for the isolated O atoms is

$$H_1 = \sum_i [\epsilon_p \sum_\sigma o^\dagger_{i,\sigma} o_{i,\sigma} + U_{pp}(1 - o^\dagger_{i\uparrow} o_{i\uparrow})(1 - o^\dagger_{i\downarrow} o_{i\downarrow})], \tag{4}$$

with $i \in \{x, y, z\}$. The Hamiltonian $H_2$ is

$$H_2 = \sum_{\sigma} [\epsilon_d + h(\frac{1}{2} + \sigma_{\acute{z}})] X^\dagger_\sigma X_\sigma + \sum_{\sigma} [\epsilon_d + h(\frac{1}{2} - \sigma_{\acute{z}})] Z^\dagger_\sigma Z_\sigma, \tag{5}$$

where $h$ is the exchange energy term that takes into account the opposite magnetization of the two $Mn^{4+}$ sites. The Hubbard correlation term is absent in $H_2$, but in the calculation we limit the Hilbert space by disregarding states with doubly occupied $X$ or $Z$ orbitals.

In our model we have chosen to neglect the electrostatic contribution to the crystal field in order to avoid the proliferation of free parameters. To estimate the severity of the neglect of such a contribution we have calculated the electronic structure of the $Sr_2MnO_4$ system using the `WIEN2k` package [24], which expands the potential within the muffin-tin spheres as a sum over spherical harmonics. Such a potential accounts for all the charges of the system. The Mn $3d$ shell was frozen in order to remove its contribution from the non-spherical part of the potential, since this contribution is already accounted for in our model. From the expansion coefficients obtained from a self-consistent calculation one can calculate the contribution to the crystal field for a localised orbital in terms of the radial integrals [25] of the product of the orbital density times the spherical harmonics coefficients. For the $3d$ shell the radial integration is not well defined because the orbitals extend non-negligibly outside the muffin-tin sphere. We can still make an estimate for a lower bound of the crystal field contribution in terms of the spherical harmonics expansion coefficients at a radius $r_{3d}$, which is chosen as the average radius for a $3d$ orbital in the isolated atom. We have found a small value ($\simeq$0.1 eV). The real value is larger because the $3d$ orbitals leak outside the muffin-tin sphere in regions where the perturbation of the neighbouring ions is stronger. However, the estimate of an upper bound is more difficult since it is not conceptually clear what exactly counts as a $3d$ orbital, outside the muffin-tin sphere.

## 3 Choice of parameters

The parameters for the atomic Hamiltonian $H_a$, which are the spin-orbit interactions and Slater integrals — except for the monopole terms which are strongly screened — have been obtained using Cowan's Hartree-Fock code [26], averaging the values for the $Mn^{3+}$ and $Mn^{4+}$ configurations. The atomic parameters are listed in Table 1. We apply scaling factors of 0.75 and 0.8 to the $dd$ and $pd$ Slater integrals, respectively, as is common practice to obtain effective Slater integrals for correlated transition metal systems [20]. For $F^0_{dd}$ we start from the estimated $U_{dd}$ of $\sim$5 eV from previous studies [21] based on spectroscopic data. Considering a starting configuration $t^3_{2g\downarrow} e^1_{g\downarrow}$ and adding two extra electrons, we obtain $t^3_{2g\downarrow} e^2_{g\downarrow} t^1_{2g\uparrow}$. Therefore, the experimental $U_{dd}$ is the interaction between a $t_{2g\uparrow}$ and $e_{g\downarrow}$ electron,

$$U_{dd} = F^0_{dd} - 4/49\, F^2_{dd} - 2/147\, F^4_{dd}, \tag{6}$$

**Table 1.** Calculated atomic Hartree-Fock values [26] for the configuration averaged Slater integrals and spin-orbit interactions (in eV).

| Configuration | $F^2_{dd}$ | $F^4_{dd}$ | $\zeta_{3d}$ | $F^2_{pd}$ | $G^1_{pd}$ | $G^3_{pd}$ | $\zeta_{2p}$ | $F^0_{dd}$ | $U_{pd}$ |
|---|---|---|---|---|---|---|---|---|---|
| Ground state | 8.94 | 5.62 | 0.051 | 5.86 | 4.38 | 2.5 | – | 5.7 | $1.1U_{dd}$ |
| Excited state | 9.53 | 5.98 | 0.063 | 5.86 | 4.38 | 2.5 | 6.85 | 5.7 | $1.1U_{dd}$ |

from which $F^0_{dd}$ is deduced.

The hopping parameter $t$ is estimated to be 1.8 eV and $U_{pp}$ is estimated to be 5 eV. The bare energy $\epsilon_p$ of the oxygen orbitals is deduced from the charge-transfer energy $\Delta = 4$ eV. This experimental parameter is defined as the energy to transfer an electron from the oxygen onto a bare Mn atom (in the absence of hybridization). Therefore,

$$\begin{aligned}\epsilon_p = -\Delta + n_d F^0_{dd} + 6F^0_{pd} - 14/49\, F^2_{dd} - 14/49\, F^4_{dd} \\ - 2/5\, G^1_{pd} - 9/35\, G^3_{pd} + (2 - n_p)U_{pp} + \delta_{\rm hyb},\end{aligned} \tag{7}$$

where $n_d$ and $n_p$ are the average occupation numbers of the Mn $3d$ and O $2p$ shell, respectively, in the ground state of the model Hamiltonian and $\delta_{\rm hyb}$ is the residual energy shift of the oxygen orbitals when we consider hybridization with inactive sites only. The value that we find is $\epsilon_p =$ 54.9 eV. Of course, such a large energy value is not referenced to the vacuum level but to a bare $3d$ state with zero occupancy. The spin-magnetization parameter $h$ for the $Mn^{4+}$ sites is 2.5 eV in the case of full spin ordering. The energy of the bare orbitals $X$ and $Z$ is

$$\epsilon_d = \epsilon_p + \Delta + \delta_d\,, \tag{8}$$

where $\delta_d$ is allowed to take values of $\sim$1 eV, which accounts for charge separation between the sites and an additional effective ligand field that compensates for the incomplete inclusion of the hybridization for the $X$ and $Z$ orbitals in the model. The spin-quantization axis $\acute{z}$ in equation (9), which fixes the orientation of the magnetization for the $Mn^{4+}$ sites, lies in the (001) plane and we have tested several different orientations.

## 4 Results

Figure 2 shows the experimental SXRD spectrum for the $(\frac{1}{4}, \frac{1}{4}, 0)$ diffraction across the Mn $L_{2,3}$ edges together with our best fit for the OO spectra, which was obtained with a hybridization reduction factor $g = 0.7$ and a $Mn^{4+}$ energy term $\delta_d = 0.8$ eV along two different magnetization directions. The reflectivity is calculated as the squared OO scattering factor divided by the absorption of the sample [17]. The absorption is calculated as a stoichiometric average of the $La_{0.5}Sr_{1.5}MnO_4$ elemental absorption. The absorption for Mn is obtained using the experimental absorption measured for $La_{0.5}Sr_{1.5}MnO_4$ at the $L_{2,3}$ absorption edges [17] and joining it with the tabulated values. The experimental spectrum has been measured at 134 K [17]. In the calculation the Hilbert space of the

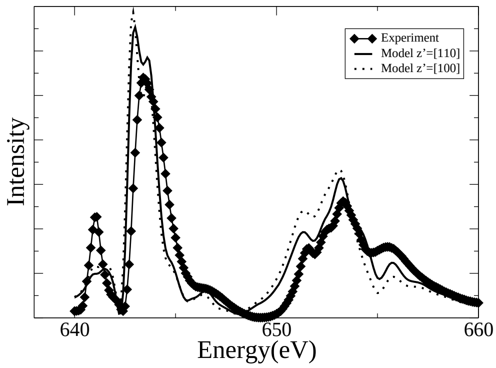


**Fig. 2.** Experimental SXRD OO spectrum recorded with $\sigma$ polarised incident light and without polarisation analysis (dashes with diamonds) together with the calculated spectra for optimised JT distortion ($g = 0.7$) and spin correlation ($h = 2.5$ eV) with the magnetisation along [100] (dotted line) and [110] (solid line). These parameter values result in $3z^2 - r^2/3x^2 - r^2$ ordering for the $e_g$ electron, and result for the alternative ordering is shown in Figure 3.

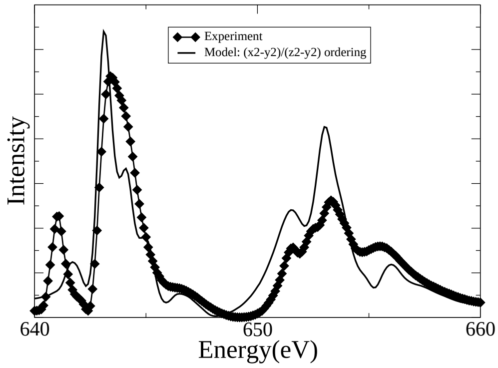


**Fig. 3.** Comparison for the $x^2 - y^2/z^2 - y^2$ ordering of the $e_g$ electron (solid line) with experiment (dashes with diamonds).

ground-state configuration and the excited-state configuration (with a $2p$ hole and an extra electron in the valence band) have been fully expanded with the constraint that there are between 8 and 12 electrons in the $Mn^{4+}$ $2p$ and $3d$ shells, and zero or one electron in each of the $X$ and $Z$ orbitals. The scattering factors are calculated in the dipole approximation using a Lorentzian broadening of $\Gamma = 0.45$ (0.55) eV for the $L_3$ ($L_2$) edge. The best fit is found for a [110] magnetisation direction. However, the dependence of the intensity on the magnetisation along [100] and [110] is not strong enough to allow a definitive assignment of the magnetisation axis. Staub et al. [8] found a magnetisation axis of $\sim 10^\circ \pm 5^\circ$ from [100] whereas Stojic et al. [7] determined a magnetisation axis of [110] based on the results of Staub et al. [8]. The differences between the assignment in the present work and the results of Staub et al. are most likely due to the assignments being made above $T_N$ in the present work and below $T_N$ in the work of Staub et al.

Our calculation reproduces all the spectral features of the experimental data in Figure 2. It is interesting to study the behaviour of the system as a function of JT distortion. Going from zero distortion ($g \simeq 1$) to a strong distortion ($g < 0.5$) we observe that the $L_3$ peak is already dominant for a very small distortion ($g \simeq 1$), while at lower $g$ values it loses intensity compared to the $L_2$ peak. This result is very different from previous analyses based on simple ligand-field models [27] which predict a direct relation between the $L_3$ main peak intensity and the JT distortion.

The simple ligand-field model most likely fails in this respect because it cannot account for the magnetic correlations between Mn ions. In our system such correlations are strongly anisotropic, being ferromagnetic along the segments of the zig-zag and anti-ferromagnetic in the perpendicular direction. This has a strong influence on the Mn $3d$ orbitals due to the superexchange mechanism [28]. Another reason why our model yields different results than the ligand-field model is because the resonant diffraction is sensitive to the differences in the scattering factor for different polarisations. These differences depend not only on the one-particle energy shifts, but also (reasoning in terms of one-particle Green functions) on the spectral-weight transfer due to the hybridization, which is neglected in ligand-field calculations.

In Figure 4, the dash-dotted line shows a calculation performed with isotropic magnetic correlation

$$H_2 = \sum_\sigma [\epsilon_d + h(\frac{1}{2} + \sigma_{\hat{z}})] X^\dagger_\sigma X_\sigma + \sum_\sigma [\epsilon_d + h(\frac{1}{2} + \sigma_{\hat{z}})] Z^\dagger_\sigma Z_\sigma, \quad (9)$$

and a small JT distortion ($g = 0.9$). We observe that in this case the OO diffraction intensity at $L_3$ is low. This drop in the $L_3$ intensity in the case of the ferromagnetic $MnO_2$ plane has been observed experimentally [29] in the study of the $LaSr_2Mn_2O_7$ system.

Analysing the one-particle Green function for the ground state we find that in our model the $e_g$ electron dwells for only 15% on the $Mn^{4+}$ site. This means a very pronounced charge separation of 0.7 electrons. However, this should not be directly compared to SCF ab-initio results since screening processes are usually very effective in solids.

We also find that the occupied $e_g$ orbital at the $Mn^{3+}$ site has $3z^2 - r^2/3x^2 - r^2$ ordering. This result contradicts the interpretation of the experimental X-ray magnetic linear dichroism (XMLD) at the Mn $L_{2,3}$ edges by Huang et al. [30] and also the SXRD analysis of Wilkins et al. [19], but agrees with recent quantum Monte Carlo simulations [31]. In order to compare the two alternatives we show in Figure 3 the OO spectra obtained by reducing the hopping along the zig-zag segment with a factor 0.7 and also reducing with the same factor the hopping to and from the out-of-plane oxygen ions. This results in an electronic structure where the $e_g$ electron has an $x^2 - y^2/z^2 - y^2$ ordering ($y$ being parallel to the $c$ axis). It is clear that the OO fit is better for the $3z^2 - r^2/3x^2 - r^2$ ordering (Fig. 1), although the differences are not dramatic enough to provide a definitive answer.

The assignment of the $z^2 - y^2/x^2 - y^2$ ordering in the SXRD work is based on a comparison of the OO energy dependence with ligand-field calculations, but the

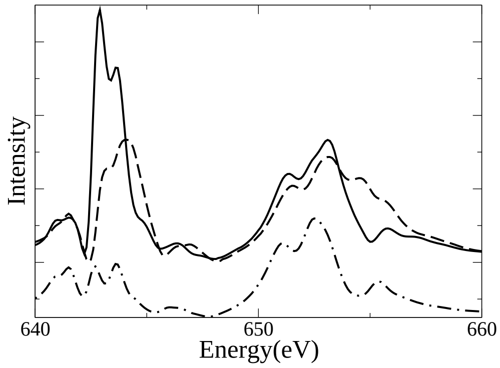


**Fig. 4.** Calculated SXRD OO spectrum for different values of the JT distortion and spin correlation parameter. The solid line is for $g = 0.7$ and $h = 2.5$ eV (as in Fig. 1). The dashed line is for $g = 0.85$ and $h = 1.25$ eV. The dash-dotted line has been obtained with $g = 0.9$ and ferromagnetic alignment of the Mn sites.

distinction between both symmetries seems to be difficult to establish [19]. The XMLD results exhibited a stronger absorption for in-plane linear polarization than for out-of-plane polarization, from which it was claimed that the occupied $e_g$ orbital has $z^2 - y^2/x^2 - y^2$ ordering. However, the work of Huang et al. [30] is based on surface sensitive X-ray absorption measurements as opposed to the bulk sensitive technique of SXRD, which might explain the difference.

A possible way to reduce the inconclusiveness of the fitted electronic structure has been explored by Wilkins et al. [19] who fitted simultaneously, below the Néel temperature, both the OO and the magnetic diffraction spectra. The magnetic diffraction spectrum that we have calculated using our model is very simple. It consists of a sharp $L_3$ peak and a small $L_2$ peak. This spectra remains qualitatively the same for all the parameter space that we have tested in the calculations reported in this work. Instead, the experimental spectra [19,29] is richer in structure and shows two main peaks at the $L_3$. The fact that these spectral features are not reproduced by our model renders the fit meaningless. Similar problems have been encounter by Wilkins et al. [19] fitting the $La_{0.5}Sr_{1.5}MnO_4$ system, for which the authors used a huge splitting ($\sim$1.4 eV) of the $t_{2g}$ band, thus obtaining two main $L_3$ peaks in the magnetic spectra. For the $LaSr_2Mn_2O_7$ [29] system instead, to explain the second main magnetic $L_3$ peak, which appears at lower energy, they advanced the hypothesis that $Mn^{2+}$ ions may be present in the system. We agree with these authors in the sense that we think that some unusual or subtle phenomenon occurs in the appearance of the low-energy part of the $L_3$ resonance and we are proceeding in a complementary direction, trying to add some missing terms, which we have neglected in the framework of this study, to the model Hamiltonian. This will be the subject of future work.

For $0.6 < g < 1$ the magnetization of the $Mn^{3+}$ site is parallel to that of the $Mn^{4+}$ site, which lies along the $x$ direction. For $g$ values below 0.6 the magnetization between the two sites is anti-parallel. What happens is that the $e_g$ orbital, lying along the $3x^2 - r^2$ direction, aligns its spin parallel to that of the $Mn^{3+}$ atom which is in the $z$ direction because for low values of $g$ the effective hopping on the $X$ orbital becomes weaker than on the $Z$ orbital. However, this phenomenon could be a coincidence since the model neglects $t_{2g}$ hybridization, which always gives an antiferromagnetic coupling with the $Z$ orbital. In any case, beyond such a magnetization-reversal threshold, the $L_3$ main peak is strongly enhanced compared to the $L_2$ and shifts to lower energy by $\sim$1.5 eV. This behaviour resembles the case of $Pr_{0.6}Ca_{0.4}MnO_3$ below $T_N$ [32]. It is then interesting to determine the effects of a reduction in the spin correlations. Our model, in particular the term $H_2$ in equation (9), considers a well-established spin order and is simplified by using symmetrised orbitals. A way to mimic the reduction of the spin correlations, without losing the simplicity of the model, is by reducing the value of $h$ in equation (9). In Figure 4, the dashed line shows the diffraction spectra for reduced values of the distortion ($g = 0.85$) and the spin correlation ($h = 1.25$ eV). The solid line gives the optimal fit to the experimental data (from Fig. 2). The change in peak heights reproduces the experimental behaviour between $T_{OO}$ and $T_N$ [17], i.e. the main $L_3$ peak loses intensity and the shoulders at low and high energy of the $L_2$ peak gain in intensity.

## 5 Conclusion

The SXRD of the orbital ordering in the half-doped manganite $La_{0.5}Sr_{1.5}MnO_4$ has been analysed using many-body cluster calculations. The dependence of the calculated orbital ordering SXRD peak intensities on the Jahn-Teller distortions is very different — if not completely opposite — to those found using ligand-field calculations, which cannot account for correlations between the spins of neighbouring Mn sites. In the many-body cluster calculations a central $Mn^{3+}$ site hybridizes with the first shell of neighbouring O sites. In turn, the O sites hybridize with the neighbouring $Mn^{4+}$ sites in the $MnO_2$ plane. The experimental spectrum at 134 K has been reproduced with good agreement, using a slight distortion of the planar O sites and by assuming a strong local magnetic correlation between Mn sites. The temperature dependence of the spectra for $T_N < T < T_{OO}$ has been reproduced by reducing simultaneously the distortion of the O sites and the spin correlation. It is not possible to reproduce the temperature dependence of the spectra between $T_N < T < T_{OO}$ by simply reducing the O distortion. These calculations show that between $T_N < T < T_{OO}$ the in-plane spin correlation is an important factor in the orbital ordering and its importance increases with the O distortion. Also a pronounced charge separation between the two Mn sites is found.

We thank the ESRF computing service for computation of the spectra, in particular Wolf Dieter Klotz and Gaby Forstner for taking care of computer clusters and grid computing.

## References


1. J.B. Goodenough, Phys. Rev. **100**, 564 (1955)
2. P.G. Radaelli, D.E. Cox, M. Marezio, S.-W. Cheong, Phys. Rev. B **55**, 3015 (1997)
3. T. Mutou, H. Kontani, Phys. Rev. Lett. **83**, 3685 (1999)
4. D. Khomskii, J. van den Brink, Phys. Rev. Lett. **85**, 3329 (2000)
5. T. Hotta, E. Dagotto, H. Koizumi, Y. Takada, Phys. Rev. Lett. **86**, 2478 (2001)
6. A. Daoud-Aladine, J. Rodriguez-Carvajal, L. Pinsard-Gaudart, M.T. Fernández-Diaz, A. Revcolevschi, Phys. Rev. Lett. **89**, 097205 (2002)
7. N. Stojic, N. Binggeli, M. Altarelli, Phys. Rev. B **72**, 104108 (2005)
8. U. Staub, V. Scagnoli, A.M. Mulders, K. Katsumata, Z. Honda, H. Grimmer, M. Horisberger, J.-M. Tonnerre, Phys. Rev. B **71**, 214421 (2005)
9. I.V. Solovyev, K. Terakura, Phys. Rev. Lett. **83**, 2825 (1999)
10. I.V. Solovyev, Phys. Rev. Lett. **91**, 177201 (2003)
11. Y. Murakami, H. Kawada, H. Kawata, M. Tanaka, T. Arima, Y. Moritomo, Y. Tokura, Phys. Rev. Lett. **80**, 1932 (1998)
12. S. Ishihara, S. Maekawa, Phys. Rev. Lett. **80**, 3799 (1998); S. Ishihara, S. Maekawa, Phys. Rev. B **58**, 13442 (1998)
13. M. Fabrizio, M. Altarelli, M. Benfatto, Phys. Rev. Lett. **80**, 3400 (1998)
14. I.S. Elfimov, V.I. Anisimov, G.A. Sawatzky, Phys. Rev. Lett. **82**, 4264 (1999)
15. P. Benedetti, J. van den Brink, E. Pavarini, A. Vigliante, P. Wochner, Phys. Rev. B **63**, 060408 (2001)
16. M. Benfatto, Y. Joly, C.R. Natoli, Phys. Rev. Lett. **83**, 636 (1999)
17. S.S. Dhesi, A. Mirone, C. Nadai, P. Ohresser, P. Bencok, N.B. Brookes, P. Reutler, A. Revcolevschi, A. Tagliaferri, O. Toulemonde, G. van der Laan, Phys. Rev. Lett. **92**, 056403 (2004)
18. S.B. Wilkins, P.D. Spencer, P.D. Hatton, S.P. Collins, M.D. Roper, D. Prabhakaran, A.T. Boothroyd, Phys. Rev. Lett. **91**, 167205 (2003)
19. S.B. Wilkins, N. Stojic, T.A.W. Beale, N. Binggeli, C.W.M. Castleton, P. Bencok, D. Prabhakaran, A.T. Boothroyd, P.D. Hatton, M. Altarelli, Phys. Rev. B **71**, 245102 (2005)
20. G. van der Laan, B.T. Thole, Phys. Rev. B **43**, 13401 (1991)
21. T. Mizokawa, A. Fujimori, Phys. Rev. B **56**, 493 (1997)
22. P. Mahadevan, K. Terakura, D.D. Sarma, Phys. Rev. Lett. **87**, 066404 (2001)
23. G. Subías, J. García, M.G. Proietti, J. Blasco, Phys. Rev. B **56**, 8183 (1997)
24. P. Blaha, K. Schwarz, G.K.H. Madsen, D. Kvasnicka, J. Luitz, `WIEN2k`, *An Augmented Plane Wave + Local Orbitals Program for Calculating Crystal Properties*, Karlheinz Schwarz, Techn. Universität Wien, Austria, 2001
25. P. Novak, Phys. Stat. Sol. B **198**, 729 (1996)
26. R.D. Cowan, *The Theory of Atomic Structure and Spectra* (University of California Press, Berkeley, 1981)
27. C.W.M. Castleton, M. Altarelli, Phys. Rev. B **62**, 1033 (2000)
28. K.I. Kugel, D.I. Khomskii, Sov. Phys. Uspekhi **25**, 231 (1982)
29. S.B. Wilkins, N. Stojic, T.A.W. Beale, N. Binggeli, P. Bencok, S. Stanescu, J.F. Mitchell, P. Abbamonte, P.D. Hatton, M. Altarelli, e-print `arXiv:cond-mat/0412435`
30. D.J. Huang, W.B. Wu, G.Y. Guo, H.-J. Lin, T.Y. Hou, C.F. Chang, C.T. Chen, A. Fujimori, T. Kimura, H.B. Huang, A. Tanaka, T. Jo, Phys. Rev. Lett. **92**, 087202 (2004)
31. M. Daghofer, A.M. Oleś, D.R. Neuber, W. von der Linden, Phys. Rev. B **73**, 104451 (2006)
32. K.T. Thomas, J.P. Hill, S. Grenier, Y.-J. Kim, P. Abbamonte, L. Venema, A. Rusydi, Y. Tomioka, Y. Tokura, D.F. McMorrow, G. Sawatazky, M. van Veenendaal, Phys. Rev. Lett. **92**, 237204 (2004)